MITR IS A SWITH THAT PROMOTES OSTEOGENESIS AND INHIBITS ADIPOGENESIS OF MESENCHYMAL STEM CELLS BY INACTIVATING PPARγ-2

Ya-Huey Chen[2,3], Fang-Ling Yeh[2,3], , Su-Peng Yeh[6], Haou-Tzong Ma[4], Shih-Chieh Hung[8],

Mien-Chie Hung[1,2,3,7] and Long-Yuan Li[1, 2,3,4,5]

From Center for Molecular Medicine, China Medical University Hospital, Taichung 40447, Taiwan[2]; Graduate Institute of Cancer Biology [3], Cancer Biology and Drug Discovery Ph.D. Program[4], China Medical University, Taichung 40402, Taiwan; Department of Biotechnology, Asia University, Taichung 41354, Taiwan[5]; Division of Hematology and Oncology, Department of Medicine, China Medical University Hospital, Taichung 40447, Taiwan[6]; Department of Molecular and Cellular Oncology, The University of Texas M.D. Anderson Cancer Center, Houston, Texas 77030, USA[7]; Department of Surgery, School of Medicine, National Yang-Ming University, Taipei, Taiwan[8]

Running title: MITR is a switch for osteogenesis of MSCs

[1]Address correspondence to: Mien-Chie Hung, Department of Molecular and Cellular Oncology, The University of Texas MD Anderson Cancer Center, 1515 Holcombe Blvd, Houston, TX 77030, USA. Tel.: +1 713 792 3668; Fax: +1 713 794 3270; E-mail: mhung@mdanderson.org; or Long-Yuan Li, Center for Molecular Medicine and Graduate Institute of Cancer Biology, China Medical University & Hospital, Taichung 40447, Taiwan. Tel.: +886 4 22052121; Fax: +886 4 22333496, E-mail: lyl@mail.cmu.edu.tw

EZH2, a catalytic subunit of Polycomb repressive complex 2 (PRC2), is a histone lysine methyltransferase (HKMT) that methylates lysine 27 of histone H3, resulting in gene silencing. It has been shown that EZH2 plays a pivotal role in fostering self-renewal and inhibiting the differentiation of embryonic stem cells. Mesenchymal stem cells (MSCs) can be induced to differentiate into adipogenic and osteogenic lineages, which are mutually exclusive. However, it is not clear whether the molecular events of EZH2-mediated epigenetic silencing may coordinate differentiation between osteoblasts and adipocytes. Disruption of the balance between adipogenesis and osteogenesis is associated with many diseases; thus, identifying a switch that determines the MSC's fate is critical. In this study, we used EZH2-ChIP-on-chip assay to identify differential EZH2 targets in the two differentiation stages on a genome-wide scale. After validating the targets, we found that MITR/HDAC9c was expressed in osteoblasts while greatly decreased in adipocytes. We demonstrated that MITR plays a crucial role in the acceleration of MSC osteogenesis and attenuation of MSC adipogenesis through interaction with PPARγ-2 in the nucleus of osteoblasts, which interrupts PPARγ-2 activity and prevents adipogenesis. Together, our results demonstrated that MITR plays a master switch role to balance osteogenic and adipogenic differentiation of MSCs through regulation of PPARγ-2 transcriptional activity.

Osteoporosis and obesity, major public health problems of body composition, have been prevalent during the last three decades. Clinically, an increase in bone mass reduction has been observed in age-associated osteoporosis, which is accompanied by an accumulation of adipose tissue in bone marrow

1

(1). Bone and fat are composed of osteoblasts and adipocytes respectively, both of which are derived from multipotent bone-marrow mesenchymal stem cells (MSCs) (2,3). Furthermore, the differentiation of adipogenic and osteogenic lineages is mutually exclusive. Disruption of the balance between MSC osteoblast and adipocyte differentiation is associated with various human diseases (3-5).

Several transcription factors such as RUNX2 and Osterix regulate osteogenesis (6,7). Overexpression of RUNX2 promotes differentiation of MSCs into osteoblasts (8). PPARγ-2, a member of the nuclear-receptor superfamily, is required for adipogenesis (9). Forced expression of PPARγ-2 is sufficient to induce differentiation of fibroblasts into adipocytes (10), and no known factors are able to stimulate adipogenesis in the absence of PPARγ-2. In addition, multipotent stem cells contain multiple key maternally inherited transcriptional factors that maintain the pluripotency, including epigenetic factors for histone modifications, such as the Polycomb group (PcG) proteins EZH2 (Enhancer of Zeste homolog) and EED (Embryonic Ectoderm Development)(11).

EZH2, a catalytic subunit of Polycomb repressive complex 2 (PRC2), is a histone lysine methyltransferase (HKMT) that methylates lysine 27 of histone H3, resulting in gene silencing (12-14). It has been shown that EZH2 plays a pivotal role in fostering self-renewal and inhibiting the differentiation of embryonic stem cells. However, it is not clear whether the molecular events of EZH2-mediated epigenetic silencing may coordinate differentiation between osteoblasts and adipocytes. Since the

differentiation of adipogenesis and osteogenesis lineages is mutually exclusive, we hypothesize that if EZH2 binds to pro-osteogenic gene promoters and inhibits pro-osteogenic gene expression, MSCs will differentiate into adipocytes. Vice versa, if EZH2 binds to pro-adipogenic gene promoters, MSCs will differentiate into osteoblasts. Therefore, to gain insight into the molecular mechanisms of MSC differentiation into adipocytes and osteoblasts, we used genome-wide EZH2-ChIP-on-chip assay to identify differential targets of EZH2 in these two differentiation stages. After narrowing down and validating the targets, interestingly, myocyte enhancer factor-2 interacting transcriptional repressor (MITR) (also named Histone Deacetylase 9c (HDAC9c)) (15) was singled out as low-expressing in adipocytes and high in osteoblasts. We therefore focused on the EZH2-target gene MITR in adipocytes to further characterize its functions in osteogenesis and adipogenesis of human MSCs. In the current study, we demonstrated that MITR plays a crucial role in the acceleration of MSC osteogenesis and attenuation of MSC adipogenesis through interaction with PPARγ-2, which interrupts PPARγ-2 transcriptional activity resulting in attenuation of adipogenesis and acceleration of osteogenesis. Together, our results demonstrated that MITR plays a switch role to balance osteogenic and adipogenic differentiation of MSCs through regulation of PPARγ-2 transcriptional activity.

Experimental Procedures

Cell culture and differentiation of osteoblasts and adipocytes- Human mesenchymal stem cell

line 3A6 (16) was maintained in low glucose DMEM (Gibco BRL) with 10 % fetal bovine serum (FBS). For adipocyte differentiation, human mesenhcymal stem cell line 3A6 and primary human mesenchymal stem cells (denoted as pMSC) were cultured in low glucose DMEM with 10 % FBS supplemented with 10^{-7} M dexamethasone, 50 μg/ml ascorbic acid-2 phosphate, and 50 μM indomethacin, 10 μg/ml insulin, and 0.45 mM 3-isobutyl-1-methyl-xanthine. Osteoblast differentiation was induced with low glucose DMEM containing 10 % FBS, 10^{-8} M dexamethasone, 50 μg/ml ascorbic acid-2 phosphate, and 10 mM beta glycerophosphate. The differentiation medium was replaced every 3 days during differentiation period (16-19).

Alizarin Red S and Oil Red O staining- Alizarin red S (Sigma) staining for osteogenic differentiated cells, Oil red O (Sigma) staining for adipogenic differentiated cells and quantification of both stainings were performed as previously described (16-19).

ChIP-on-chip for EZH2- Mesenchymal stem cells 3A6 were differentiated into osteoblasts and adipocytes for 7 days and then 10^9 cells were harvested for the ChIP-on-chip assay. The procedure was based on the manufacturer's instructions (NimbleGen Company). The results from NimbleGen promoter array were analyzed by the SignalMap^{TM} software. The EZH2 antibody was purchased from Cell Signaling.

Real-time reverse transcription- PCR- Total RNA was isolated using Trizol (Invitrogen) according to the manufacturer's instructions. After total RNA isolation, cDNA was generated by SuperScript ^{TM} III reverse transcriptase (Invitrogen) and analyzed by real-time PCR

(Roche, LightCycler® 480) with Human Universal ProbeLibrary set. All reaction products were normalized to the mRNA expression level of GAPDH. PCR primer sets used are listed in the Supplemental Table 1.

*Protein extraction from mice tissues-*The bones and adipose tissues from hind legs and abdomen were isolated from mice and frozen in liquid nitrogen. The frozen tissues were then grinded into powder and lysed by NETN (150 mM NaCl, 1 mM EDTA, 20 mM Tris-HCl, 0.5% NP40) lysis buffer containing protease inhibitors. The protein extracts were examined by western blotting analysis.

Quantitative Chromatin immunoprecipitation (qChIP) assay- Chromatin immunoprecipitation (ChIP) assays were performed using EZ-ChIP kit (Upstate) according to the manufacturer's instructions. Specific antibodies against EZH2 (Cell Signaling), H3K27me3 (Abcam), PPARγ-2 (Abcam, ab45036), RUNX2, and MITR (Santa Cruz Biotechnology) were used for immunoprecipitation in ChIP assays. The immunoprecipitated DNA was subjected to real time PCR using Roche Cybr Green system according to the manufacturer's instructions. Data was presented as the fold enrichment of precipitated DNA relative to 2/100 dilution of input chromatin. Primers are listed in Supplemental Table 1.

Electrophoretic-Mobility Shift Assay (EMSA) assay- EMSA were performed utilizing LightShift® Chemiluminescent EMSA kit (Thermo Scientific) according to the manufacturer's instructions. Nuclear extracts were harvested after MSC differentiated into osteoblasts and adipocytes for 7 days. The 5 μg of nuclear extract was incubated with binding

3

buffer, 1 µg of poly (dIdC), and 1 pg of biotin labeled double-stranded oligonucleotides containing MITR promoter region at room temperature for 20 minutes. For the competition experiments, unlabeled cold competitive oligonucleotides were included in the reaction mixture. To verify the involvement of EZH2 in the complex, specific antibody against EZH2 (Cell Signaling) was added to the reaction mixture. Oligonucleotides that contain EZH2-bound sequence of HDAC9c promoter region were used for EMSA and listed in Supplemental Table 1.

Lentiviral infection- The lentiviral shRNA clones were purchased from National RNAi Core Facility of Academic Sinica, Taiwan. MSC 3A6 or pMSC cells were infected with vector alone (pLK0.1) lentivirus and MITR shRNA lentivirus supplemented with Polybrene (8µg/ml). Following infection, cells were differentiated into adipocytes and osteoblasts as described above.

Adenoviral infection- The cDNA of MITR (NM_014707) was cloned into adenoviral expression system (AdEasy[TM] XL adenoviral system, Strategene). MSCs were infected with either vector alone (Null adenovirus) or MITR adenovirus. The infected cells were then differentiated into adipocytes and osteoblasts as described above.

Western blotting and immunoprecipitation- Cells were harvested on ice by using NETN (150 mM NaCl, 1 mM EDTA, 20 mM Tris-HCl, 0.5% NP40) buffer supplemented with protease inhibitors and lyastes were incubated with anti-MITR antibodies (Santa Cruz Biotechnology) for overnight at 4^0C. Immune complexes were precipitated with protein A/G

(Roche Applied Science) for 3h at 4^0C. The beads were washed four times with NETN buffer. Proteins were eluted from the beads by boiling in sample buffer for 5 min, and then analyzed by electrophoresis on SDS-polyacrylamide gels, and transferred to polyvinlidene disfluoride (PVDF) membranes. Specific antibodies against RUNX2, MITR, and OPN (Santa Cruz Biotechnology), PPARγ-2 (Abcam, ab45036), and FABP4 (Cell Signaling) were used.

Cytosol and nuclear fractions- Cells were harvested on ice by using Nori (20 mM Hepes pH7.0, 10 mM KCl, 2 mM $MgCl_2$, 0.5% NP-40) buffer supplemented with protease inhibitors and homogenized for 70 strokes with a Dounce homogenizer. Samples were transferred to microcentrifuge tubes and centrifuged at 4000 rpm at 4 ^{o}C for 5 min. The resulting supernatant was centrifuged at 13,000 rpm for 20 min at 4 ^{o}C to obtain a cytosolic fraction. The cell pellets were further washed and centrifuged at top speed at 4 ^{o}C for 20 min. The pellet was resuspended in NETN lysis buffer supplemented with 1% Triton X-100, and then analyzed by immunoprecipitation/Western blotting analysis using specific antibodies.

Reporter-Gene assay- The FABP4 promoter-luciferase reporter plasmid was generated according to paper published by Rival et al. (20). The FABP4 promoter-luciferase reporter plasmid was transfected into MSCs or 293 cells together with internal control plasmid pRL-TK and indicated plasmids using lipofectamin 2000 (Invitrogen). After 24 hours, cell extracts were harvested and luciferase activity was measured by dual-luciferase reporter assay system according to the

4

manufacturer's instructions (Promega).

RESULTS

EZH2 binds to the MITR promoter and inhibits MITR expression in adipocytes but not in osteoblasts. Since epigenetic regulators for histone modification such as PcG proteins, including EZH2, are important for stem cell pluripotency, we attempted to elucidate the regulatory mechanism of EZH2 in differentiated adipocytes and osteoblasts by identifying EZH2 target genes using genome-wide ChIP-on-Chip assays. Human MSC cell line 3A6 (16) was differentiated into osteoblasts and adipocytes for seven days and analyzed for EZH2-ChIP-on-chip assays. We first showed no change in EZH2 expression before and after differentiation (Fig. 1A). Interestingly, we found 250 EZH2 target genes in adipocytes and 30 target genes in osteoblasts with no overlapping genes (Fig. 1B) using SignalMap software to analyze the binding peak in promoter region and looked for binding peaks with a FDR (false discovery rate) score smaller than 0.2. In addition, to search for potential genes that might trigger differential balance of osteogenesis and adipogenesis, we looked for cellular and organic development /differentiation-related genes along with genes that are also differentially expressed between adipocytes and osteoblasts. Interestingly, based on the criteria, myocyte enhancer factor-2 interacting transcriptional repressor (MITR) (also named Histone Deacetylase 9c (HDAC9c)) was singled out. A representative set of data is shown, demonstrating that the mRNA expression level of MITR was high in osteoblasts and low in

adipocytes compared with undifferentiated MSCs (Fig. 1C). Western blotting analysis supported the differential expression (Fig. 1D). Consistent with these results, we also observed that MITR expression was higher in bones than in adipose tissues isolated from three mice (Fig. 1E). These results suggest that MITR is highly expressed in both differentiated osteoblasts from MSC and bone tissues from mice but not in adipocytes and adipose tissues. Moreover, quantitative Chromatin immunoprecipitation (qChIP) assays further demonstrated detectable binding of EZH2 and of the tri-methylated histone H3 at lysine 27 (H3K27me3) to the MITR promoter in adipocytes but not in osteoblasts or undifferentiated MSCs (Fig. 1F and G). To further support the qChIP data that EZH2 binds to MITR promoter, electrophoretic mobility shift assay (EMSA) was carried out and showed that binding of EZH2 to MITR promoter in adipocytes is much stronger than in osteoblasts (Fig. 1H, left panel). In addition, binding of EZH2 to MITR promoter in adipocyte was declined as demonstrated by a competition assay using 1000-fold of MITR cold probe and EZH2 antibody (Fig. 1H, right panel). Together, these results suggest that EZH2 binds to and methylates lysine 27 of histone H3 at MITR promoter region to inhibit expression of MITR in MSCs and adipocytes. However, after osteoblast differentiation, binding of EZH2 to the MITR promoter is repressed and therefore MITR expression is de-repressed, suggesting MITR might be a pro-osteogenic regulator.

Expression of MITR enhances osteogenesis and inhibits adipogenesis. MITR shares about 50% homology with the N-terminus of HDAC4

5

and HDAC5, and is missing the catalytic domain. Without a catalytic domain, MITR cannot function as a deacetylase. Instead, it was shown that MITR, by interaction with MEF2 (CaMK/14-3-3) is involved in muscle differentiation (15,21,22). It has also been reported that inhibition of HDAC1 enhances adipogenesis (23). Thus, we next investigated whether MITR plays a role in MSC differentiation into adipocytes and osteoblasts. We utilized two lentiviral based shRNAs to specifically knockdown the expression of MITR in MSCs. The knockdown efficiency was examined using western blotting analysis (Fig. S1). As shown in Fig. 2A and B, knockdown of MITR using shRNA inhibited osteoblast differentiation induced by osteogenic induction media as revealed by reduced Alizarin Red S staining (at OD_{450}), a measure for osteogenic differentiation (Fig. 2A), and decreased expression of osteoblast differentiation markers RUNX2 and osteopontin (OPN) (Fig. 2B, lane 5), suggesting that MITR is required for osteoblast differentiation. Interestingly, knockdown of MITR expression enhances adipocyte differentiation of MSCs treated with adipogenic induction media as measured by increased Oil Red O staining (at OD_{510}), a measure for adipogenesis (Fig. 2C). Cells were stained with Oil Red O to visualize intracellular lipid deposition and photographed. (Fig. 2C) The results seem to suggest that MITR expression plays opposing roles for adipocyte and osteoblast differentiation, namely, inhibiting adipocyte differentiation, and being required for osteoblast differentiation. To further validate this notion, we generated an adenovirus based delivery system to increase MITR expression in

MSCs (Fig. 3A). Ectopic expression of MITR enhanced osteoblasts differentiation as demonstrated by increased Alizarin Red S staining and the quantification results are shown (Fig. 3B). Supporting this notion, Oil Red O staining and quantification results showed that ectopic expression of MITR suppressed adipogenesis, i.e., MITR expression inhibited adipocyte differentiation induced by adipogenic induction media (Fig. 3C). Together the results suggest that EZH2-regulated MITR plays a switch role to balance osteogenesis and adipogenesis of MSCs.

MITR also promotes osteogenesis in multiple primary human MSCs. To further validate the role of MITR during osteogenesis, we assessed MITR protein expression during differentiation of primary human bone marrow-derived MSC cultures into osteoblasts and adipocytes. Under differentiation conditions, osteogenesis and adipogenesis were accompanied by increased and decreased MITR expression, respectively, as compared with the parental primary human MSCs (Fig. S2A) We used lentiviral based shRNA to attenuate MITR expression and observed that the expression of the osteoblast differentiation marker OPN was decreased in primary MSCs treated with MITR shRNA (Fig. 4A). In addition, inhibition of MITR repressed osteogenic differentiation as shown by decreased Alizarin Red S staining (Fig. 4B). Alternatively, using the adenoviral delivery system to enhance MITR expression in primary MSCs (Fig. 4C) promoted osteogenesis as shown by elevated Alizarin Red S staining (Fig. 4D) and OPN expression (Fig. 4C). Similar results were also observed in two other primary MSCs (Fig. S2B-I), indicating that three

6

primary MSC cultures behaved similarly to the MSC cell line (Figs. 2 and 3). These data suggest that MITR may play an important role in regulation of primary human MSCs differentiation into osteoblasts.

MITR attenuates PPARγ-2 transcriptional activity through association in osteoblastic nucleus. Recent studies have shown that histone deacetylase (HDAC) family members are able to interact with transcription factors and repress their activity (24,25). Since PPARγ-2 and RUNX2 are important transcription factors promoting adipogenesis and osteogenesis, respectively, we thus asked whether the enhanced MITR expression in osteoblasts might interact with PPARγ-2 or RUNX2 to promote osteogenesis. Nuclear and cytosolic extracts were harvested and followed by immunoprecipitation with MITR (Fig. 5A) or PPARγ-2 (Fig. 5B) antibodies after seven days of osteogenic differentiation. The binding between MITR and PPARγ-2 both in cytosolic and nuclear extracts was then analyzed. As shown in the Figs. 5A and 5B, the MITR and PPARγ-2 complex was only detected in the nuclear extracts of osteoblasts (Fig. 5A and B) but not in the nuclear extracts of adipocytes (data not shown). On the other hand, MITR did not interact with RUNX2 in the nuclear or cytoplasmic fraction of osteoblasts (Fig. 5C). Since MITR and PPARγ-2 promoted osteogenesis and adipogenesis, respectively, we asked whether the MITR and PPARγ-2 interaction might render inactivation of PPARγ-2 transcriptional activity that turns on adipocyte differentiation markers in osteoblasts. First we analyzed RNA expression level of a PPARγ-2-driven gene, fatty acid binding protein

4 (FABP4). As expected FABP4 expression level was dramatically higher in adipocytes than those in MSCs or in osteoblasts (Fig. 6A). Next, we investigated whether MITR inhibits PPARγ-2-activated FABP4 promoter activity. MSC cell line and 293 cells were transfected with human FABP4 promoter-driven luciferase reporter plasmid together with PPARγ-2 or MITR plasmids as indicated in Fig. 6B. The results showed that PPARγ-2-stimulated FABP4 promoter activity was significantly suppressed in the presence of MITR (Fig. 6B). Consistently, binding of PPARγ-2 to the human FABP4 promoter was abrogated in the presence of MITR in MSCs using quantitative-ChIP assays (Fig. 6C), revealing MITR inhibits PPARγ-2's transcriptional activity by abrogating binding of PPARγ-2 to adipocyte marker gene FABP4 promoter thus repressing its expression. In addition, we found that PPARγ-2 was recruited to its targeted-gene promoter FABP4 in adipocytes (Fig. 6D, upper panel) while RUNX2 was recruited to its targeted-gene promoter OPN in osteoblasts (Fig. 6D, lower panel). Thus, these results suggest that enhanced osteoblast differentiation may require MITR association with PPARγ-2 and inhibition of PPARγ-2's transcriptional activity along with the promotion of osteogenesis, such as through enhancing OPN gene expression by RUNX2. Taken together, we found that EZH2 bound to the MITR promoter suppressing MITR in adipocytes but not in osteoblasts. The presence of MITR in osteoblasts promoted the formation of the MITR and PPARγ-2 complex in the nucleus of osteoblasts inhibiting PPARγ-2's transcriptional activity and preventing adipocyte differentiation. Thus, MITR functions as a

transcriptional co-repressor in MSCs undergoing osteogenesis through interruption of PPARγ-2 transcriptional activity (Fig. 6E).

DISCUSSION

Accumulated evidence has demonstrated a possible role for the polycomb group (PcG) proteins in regulating tissue development and maintenance of multipotent progenitor cells (26). PRC2, which is composed of EZH2, EED, and SUZ12, is recruited to chromatin where trimethylation on lysine 27 of Histone H3 (triMeK27-H3) was catalyzed by EZH2 methyltransferase (13). We now show that EZH2 targeted and inactivated the MITR promoter in adipocytes resulting in its decreased expression, but not in osteoblasts. Furthermore, we found that EZH2-mediated epigenetic regulation of MITR plays an important role over MSC osteogenic and adipogenic lineage allocation. MITR lacks the c-terminal and catalytic domain (22); therefore, MITR does not possess intrinsic HDAC activity. MITR is classified into class IIa HDACs and expressed in a tissue-specific manner. Class II HDACs modulate cell differentiation through recruitment of different interacting partners including NF-AT3c (transcription factor required for cell differentiation and immune response), N-CoR (nuclear receptor corepressor), and HP1 (heterochromatin protein 1 and associated with the methyltransferase (27). Therefore, HDACs have powerful ability to attract partner proteins to regulate cell fate beside their own histone deacetylase function. In addition, previous studies also showed that HDAC1, HDAC3 and HDAC7 modulate

osteoblasts differentiation via modification of histone or interaction with RUNX2, respectively (28-30). Moreover, it has also been reported that MITR fused to Gal4 DNA-binding domain suppresses transcription in transient transfection assays, indicating MITR is a transcriptional repressor (15). In the current study, we demonstrate that MITR interacts with PPARγ-2 in osteoblastic nucleus to prevent from binding of PPARγ-2 to adipocyte marker gene FABP4 promoter thus repressing its expression, indicating MITR may possibly function as a transcriptional co-repressor to inhibit PPARγ-2 transcription and therefore represses adipogenesis and promotes osteogenesis of MSCs. However, it remains unclear that how MITR-bound PPARγ-2 loses its ability to bind to the target gene promoters. One of the possible mechanisms may be due to the conformational change of PPARγ-2 after binding with MITR, resulting in sheltering PPARγ-2's DNA-binding domain, thereby hindering its association with target promoters. In this regard, Suzawa et al. also found that NF-κB activated by cytokine signaling interacts with the DNA-binding domain of PPAR-γ which prevents PPAR-γ binding to target gene promoters, leading to inhibiting adipogenesis (31). These results further reveal that modulation of PPAR-γ's DNA binding ability confers another level of PPAR-γ regulation. Further systematic study is required to address this interesting issue.

Previous studies have reported that mice lacking both HDAC9 and MITR are hypersensitive to hypertrophic stimuli and spontaneously develop age-dependent cardiac hypertrophy (32). These mice are also sensitized to calcineurin signaling-mediated cardiac

8

hypertrophy, unveiling HDAC9 and MITR act as transcriptional repressor of signal-induced hypertrophic growth of cardiomyocyte (32). This phenotypic impact of HDAC9 and MITR is associated with transcription factor, myocyte enhancer factor-2. Interestingly, HDAC4-null mice showed ectopic chondrocyte hypertrophy which results in premature ossification of developing bones, a similar phenotype that is caused by constitutive expression of RUNX2 in chondrocyte (33). In addition, HDAC4 physically interacts with and suppresses RUNX2 transcriptional activity, leading to inhibitory effects on RUNX2's target genes expression and chondrocyte hypertrophy (33,34). In the current study, we found that MITR enhances osteogenesis but impedes adipogenesis of MSCs by interacting with PPARγ-2 and repressing its transcriptional activity. Together, these studies suggest that class II HDACs may fine tune a variety of cellular processes through disparate modes of action such as interacting with specific transcription factors. Moreover, multiple HDACs may involve in the delicate coordination of the same cellular process but contribute to unique functions at the different stages of cellular process. For example, during bone development, HDAC4 modulates chondrocyte hypertrophy, and MITR regulates osteoblast differentiation.

It is worthy to mention that HDAC inhibitors, such as TSA, Scriptaid and SAHA, have been shown to inhibit preadipocyte differentiation (35-37). However, HDAC inhibitors sodium butyrate and valproic acid stimulated adipogenesis of preadipocytes (23,35). Sodium butyrate and valproic acid belong to short chain fatty acid chemicals, that has previously been known to enhance adipogenesis. Thus, the opposite effect of HDAC inhibitors on adipogenesis could be attributed to the nature of HDAC inhibitors. Indeed, Olson laboratory demonstrated that sodium butyrate and valproic acid-enhanced adipogenesis was abrogated while co-treament with TSA, indicating the augmented adipogenesis resulted from the short chain fatty acid character of sodium butyrate and valproic acid instead of HDAC inhibition (35). In addition, knocking down HDAC1 using siRNA promoted preadipocyte 3T3-L1 differentiation (23). Conversely, genetic deletion of both HDAC 1 and 2 together in mouse embryonic fibroblasts blocked adipogenesis (35). Several lines of evidence have shown that HDAC1 and HDAC2 redundantly coordinate gene expression that control variety of cellular processes including differentiation (38-40). Hence, the discrepancy could be caused by the different methodologies and/or differentiation systems used in the two studies. In addition, redundancy of the two genes might also contribute to the discrepancy. Further experimental delineation is required to clarify these issues.

Interestingly, recent studies show that depletion of EZH2 leads to a severe impaired adipogenesis in primary white preadipocytes. Adipogenesis was facilitated by H3K27 methyltransferase EZH2-mediated repression of Wnt genes directly. Thus, consistent with our results, this study also highlights the importance for EZH2-mediated differentiation (41). In addition, a 14-3-3-binding protein TAZ, which is a transcriptional coactivator with PDZ-binding motif, has been shown to function as a coactivator of RUNX2 and a repressor of

9

PPARγ to inhibit PPARγ-dependent transcriptional events, suggesting TAZ may act as a molecular switch to adjust the balance between osteogenesis and adipogenesis (42). Together with our results, further investigation is required to understand how all these regulators might coordinate the two differentiation fates. Here, studying the mechanisms for MSC lineage allocation exposes the importance of epigenetic regulation, and provides an example of how a non-catalytic HDAC protein participates in MSC differentiation into osteoblasts and adipocytes.

REFERENCES

1. Pei, L., and Tontonoz, P. (2004) *The Journal of clinical investigation* **113**(6), 805-806

2. Rosen, C. J. (2008) *Cell Metab* **7**(1), 7-10

3. Rosen, C. J., and Klibanski, A. (2009) *Am J Med* **122**(5), 409-414

4. Surani, M. A., Hayashi, K., and Hajkova, P. (2007) *Cell* **128**(4), 747-762

5. Nuttall, M. E., and Gimble, J. M. (2000) *Bone* **27**(2), 177-184

6. Blair, H. C., Zaidi, M., and Schlesinger, P. H. (2002) *Biochem J* **364**(Pt 2), 329-341

7. Wagner, E. F., and Karsenty, G. (2001) *Curr Opin Genet Dev* **11**(5), 527-532

8. Ducy, P., Zhang, R., Geoffroy, V., Ridall, A. L., and Karsenty, G. (1997) *Cell* **89**(5), 747-754

9. Rosen, E. D., Walkey, C. J., Puigserver, P., and Spiegelman, B. M. (2000) *Genes & development* **14**(11), 1293-1307

10. Tontonoz, P., Hu, E., and Spiegelman, B. M. (1994) *Cell* **79**(7), 1147-1156

11. Jaiswal, R. K., Jaiswal, N., Bruder, S. P., Mbalaviele, G., Marshak, D. R., and Pittenger, M. F. (2000) *The Journal of biological chemistry* **275**(13), 9645-9652

12. Kuzmichev, A., Jenuwein, T., Tempst, P., and Reinberg, D. (2004) *Mol Cell* **14**(2), 183-193

13. Cao, R., Wang, L., Wang, H., Xia, L., Erdjument-Bromage, H., Tempst, P., Jones, R. S., and Zhang, Y. (2002) *Science* **298**(5595), 1039-1043

14. Ramsden, D., and Zhang, Y. (2003) *Nat Immunol* **4**(2), 101-103

15. Zhou, X., Richon, V. M., Rifkind, R. A., and Marks, P. A. (2000) *Proceedings of the National Academy of Sciences of the United States of America* **97**(3), 1056-1061

16. Tsai, C. C., Chen, C. L., Liu, H. C., Lee, Y. T., Wang, H. W., Hou, L. T., and Hung, S. C. (2010) *J Biomed Sci* **17**, 64

17. Hung, S. C., Chen, N. J., Hsieh, S. L., Li, H., Ma, H. L., and Lo, W. H. (2002) *Stem Cells* **20**(3), 249-258

18. Wei, Y. J., Tsai, K. S., Lin, L. C., Lee, Y. T., Chi, C. W., Chang, M. C., Tsai, T. H., and Hung, S. C. (2010) *Osteoporos Int*

19. Hung, S. C., Yang, D. M., Chang, C. F., Lin, R. J., Wang, J. S., Low-Tone Ho, L., and

Yang, W. K. (2004) *Int J Cancer* **110**(3), 313-319

20.	Rival, Y., Stennevin, A., Puech, L., Rouquette, A., Cathala, C., Lestienne, F., Dupont-Passelaigue, E., Patoiseau, J. F., Wurch, T., and Junquero, D. (2004) *J Pharmacol Exp Ther* **311**(2), 467-475

21.	Bertos, N. R., Wang, A. H., and Yang, X. J. (2001) *Biochem Cell Biol* **79**(3), 243-252

22.	Zhou, X., Marks, P. A., Rifkind, R. A., and Richon, V. M. (2001) *Proceedings of the National Academy of Sciences of the United States of America* **98**(19), 10572-10577

23.	Yoo, E. J., Chung, J. J., Choe, S. S., Kim, K. H., and Kim, J. B. (2006) *The Journal of biological chemistry* **281**(10), 6608-6615

24.	Fischle, W., Dequiedt, F., Fillion, M., Hendzel, M. J., Voelter, W., and Verdin, E. (2001) *The Journal of biological chemistry* **276**(38), 35826-35835

25.	Fischle, W., Dequiedt, F., Hendzel, M. J., Guenther, M. G., Lazar, M. A., Voelter, W., and Verdin, E. (2002) *Mol Cell* **9**(1), 45-57

26.	Ringrose, L., and Paro, R. (2004) *Annu Rev Genet* **38**, 413-443

27.	Yang, X. J., and Gregoire, S. (2005) *Mol Cell Biol* **25**(8), 2873-2884

28.	Lee, H. W., Suh, J. H., Kim, A. Y., Lee, Y. S., Park, S. Y., and Kim, J. B. (2006) *Mol Endocrinol* **20**(10), 2432-2443

29.	Schroeder, T. M., Kahler, R. A., Li, X., and Westendorf, J. J. (2004) *J Biol Chem* **279**(40), 41998-42007

30.	Jensen, E. D., Schroeder, T. M., Bailey, J., Gopalakrishnan, R., and Westendorf, J. J. (2008) *J Bone Miner Res* **23**(3), 361-372

31.	Suzawa, M., Takada, I., Yanagisawa, J., Ohtake, F., Ogawa, S., Yamauchi, T., Kadowaki, T., Takeuchi, Y., Shibuya, H., Gotoh, Y., Matsumoto, K., and Kato, S. (2003) *Nature cell biology* **5**(3), 224-230

32.	Zhang, C. L., McKinsey, T. A., Chang, S., Antos, C. L., Hill, J. A., and Olson, E. N. (2002) *Cell* **110**(4), 479-488

33.	Vega, R. B., Matsuda, K., Oh, J., Barbosa, A. C., Yang, X., Meadows, E., McAnally, J., Pomajzl, C., Shelton, J. M., Richardson, J. A., Karsenty, G., and Olson, E. N. (2004) *Cell* **119**(4), 555-566

34.	Shimizu, E., Selvamurugan, N., Westendorf, J. J., Olson, E. N., and Partridge, N. C. (2010) *The Journal of biological chemistry* **285**(13), 9616-9626

35.	Haberland, M., Carrer, M., Mokalled, M. H., Montgomery, R. L., and Olson, E. N. (2010) *The Journal of biological chemistry* **285**(19), 14663-14670

36.	Nebbioso, A., Dell'Aversana, C., Bugge, A., Sarno, R., Valente, S., Rotili, D., Manzo, F., Teti, D., Mandrup, S., Ciana, P., Maggi, A., Mai, A., Gronemeyer, H., and Altucci, L. (2010) *J Mol Endocrinol* **45**(4), 219-228

37.	Catalioto, R. M., Maggi, C. A., and Giuliani, S. (2009) *Exp Cell Res* **315**(19), 3267-3280

38.   Montgomery, R. L., Davis, C. A., Potthoff, M. J., Haberland, M., Fielitz, J., Qi, X., Hill, J. A., Richardson, J. A., and Olson, E. N. (2007) *Genes & development* **21**(14), 1790-1802

39.   Montgomery, R. L., Potthoff, M. J., Haberland, M., Qi, X., Matsuzaki, S., Humphries, K. M., Richardson, J. A., Bassel-Duby, R., and Olson, E. N. (2008) *The Journal of clinical investigation* **118**(11), 3588-3597

40.   Haberland, M., Montgomery, R. L., and Olson, E. N. (2009) *Nature reviews* **10**(1), 32-42

41.   Wang, L., Jin, Q., Lee, J. E., Su, I. H., and Ge, K. (2010) *Proceedings of the National Academy of Sciences of the United States of America* **107**(16), 7317-7322

42.   Hong, J. H., Hwang, E. S., McManus, M. T., Amsterdam, A., Tian, Y., Kalmukova, R., Mueller, E., Benjamin, T., Spiegelman, B. M., Sharp, P. A., Hopkins, N., and Yaffe, M. B. (2005) *Science* **309**(5737), 1074-1078

FOOTNOTES

The abbreviations used are: MITR, myocyte enhancer factor-2 interacting transcriptional repressor; MSCs, mesenchymal stem cells; pMSCs, primary human MSCs; FABP4, Fatty acid binding protein 4; OPN, osteopontin; ChIP, chromatin immunoprecipitation; EMSA, electrophoretic mobility shift assay.

FIGURE LEGENDS

Fig. 1. EZH2 binds to the MITR promoter and inhibits MITR expression in adipocytes but not in osteoblasts. A & B. Human mesenchymal stem cell line 3A6 (MSC) was differentiated into osteoblasts (Ost.) and adipocytes (Adi.) for seven days and analyzed for EZH2 expression by western blotting (A) and EZH2-ChIP-on-chip assays (B). The total EZH2-targeted genes in undifferentiated MSCs, adipocytes and osteoblasts are listed. C. EZH2-targeted genes were confirmed using real time RT-PCR. RNA expression in differentiated MSCs compared to parental MSCs is plotted. The data are expressed as mean ± SD. CAST, calpastatin; PHTF1, putative homeodomain transcription factor1; MITR, myocyte enhancer factor-2 interacting transcriptional repressor (also named histone

deacetylase 9 c, HDAC9c); NRG1, neuregulin; OSTF1, osteoclast stimulating factor 1; ZBTB10, zinc finger and BTB domain containing 10. D. Protein expression levels of MITR in indicated cells were analyzed using western blotting analysis with indicated antibodies. E. Protein expression levels of MITR in bone and adipose tissues from mice were examined using western blotting analysis with indicated antibodies. F & G. Binding of EZH2 and tri-methylated histone H3 at lysine 27 (H3K27me3) at MITR promoter during osteogenesis and adipogenesis were analyzed using quantitative ChIP assay. Cross-linked chromatin from MSC, Ost. or Adi. was immunoprecipitated using EZH2 (F), H3K27me3 (G) or IgG antibodies. The input and immunoprecipitated DNA were subjected to PCR (upper panels) or real time PCR (lower panels) using primers corresponding to promoter region of MITR listed in Supplemental Table 1. H. Binding of EZH2 to MITR promoter during osteogenesis and adipogenesis was analyzed using electrophoretic mobility shift assay (EMSA). Biotin labeled double-stranded oligonucleotides containing MITR promoter region was incubated with nuclear extracts harvested from differentiated osteoblasts and adipocytes (left panel). For the competition experiments, unlabeled cold competitive oligonucleotides were included in the reaction mixture. To verify the involvement of EZH2 in the complex (arrows), specific antibody against EZH2 was added to the reaction mixture (right panel). Oligonucleotides that contain EZH2-bound sequence of HDAC9c promoter region were used for EMSA and listed in Supplemental Table 1.

Fig. 2. Knocking down MITR inhibits osteogenesis and enhances adipogenesis. A. MSCs infected with MITR (shMITR-1 or -2) or control (shControl) shRNA lentiviral vectors were stained with Alizarin Red S, a measure for osteogenesis, after inducing osteoblasts differentiation for seven days. The quantification of staining was measured by spectrophotometer at 450 nm (OD_{450}) and presented as the mean $\pm$ SD. B. The expression of MITR, osteogenic markers RUNX2 and OPN, and adipogenic marker FABP4 in MSCs, osteoblasts (Ost.), adipocytes (Adi.) (lanes 1-3) or MSCs infected with indicated shRNAs viral vectors even days after inducing osteoblasts differentiation (lanes 4-5) using western blotting analysis. OPN, osteopontin; FABP4, Fatty acid binding protein 4. C. MSCs infected with indicated shRNA lentiviral vectors were stained with Oil Red O, a measure for adipogenesis, after inducing adipocytes differentiation for seven days. Cells were stained to visualize intracellular lipid deposition by phase-contrast microscopy and photographed. The quantification of staining was measured by spectrophotometer at 510 nm (OD_{510}) and presented as the mean $\pm$ SD. p-values were analyzed using Student's t-test.

Fig. 3. Expression of MITR enhances osteogenesis and attenuates adipogenesis. A. Expression of MITR in MSCs using adenoviral-based system. Ectopic expression of MITR in MSCs infected with MITR (AdMITR) or control (AdControl) adenovirus was detected by western blotting. B. MSCs infected with indicated adenovirus were stained with Alizarin Red S after inducing osteoblasts differentiation for seven days. The quantitative results for the staining measured by OD_{450} are presented as the mean $\pm$ SD. C. MSCs infected with indicated adenovirus were stained with Oil Red O

13

seven days after inducing adipocytes differentiation. Cells were stained to visualize intracellular lipid deposition by phase-contrast microscopy and photographed. The quantitative results for the staining measured by OD_{510} are presented as the mean ± SD. p-values were analyzed using Student's t-test.

Fig. 4. Knockdown of MITR inhibits osteogenesis in primary human MSCs. **A.** Examination of HDAC9c and osteogenic marker osteopontin (OPN) expression in primary human MSCs (pMSC-1) infected with MITR (shMITR) or control (shControl) shRNAs lentiviral vectors after inducing osteoblasts differentiation for seven days using western blotting analysis. B. Primary human MSCs treated as in (A) were stained with Alizarin Red S seven days after induction of osteoblast differentiation. The quantification of staining was measured by spectrophotometer at 450 nm (OD_{450}) and presented as the mean ± SD. C. Ectopic expression of MITR in primary human MSCs using adenoviral-based system. Cell extracts from pMSC-1 infected with MITR (AdMITR) or control (AdControl) adenovirus after inducing osteoblasts differentiation for seven days were analyzed using western blotting with antibodies as indicated. D. Primary human MSCs treated as in (C) were stained with Alizarin Red S seven days after induction of osteoblast differentiation. The quantification of staining was measured by spectrophotometer at 450 nm (OD_{450}) and presented as the mean ± SD. p-values were analyzed using Student's t-test.

Fig. 5. MITR interacts with PPARγ-2 in osteoblastic nucleus. A & B. Cytosolic and nuclear cells extracts were harvested after inducing osteoblasts differentiation of MSCs for seven days and immunoprecipitated with MITR antibody (A) or PPARγ-2 antibody (B) and western blotted with antibodies as indicated. MITR and PPARγ-2 complex was detected in the nuclear fraction but not in the cytosolic fraction in osteoblasts (Ost.). C. MITR does not interact with Runx2 in the nuclear or cytoplasmic fraction of osteoblasts. Cytosolic and nuclear cells extracts from MSCs treated as in (A) were immunoprecipitated with MITR antibody and western blotted with antibodies as indicated.

Fig. 6. MITR inhibits the transcriptional activity of PPARγ-2 via abrogating binding of PPARγ-2 to adipocyte marker gene FABP4 promoter. A. MSCs were differentiated into osteoblasts (Ost.) and adipocytes (Adi.) for seven days and analyzed for FABP4 RNA expression using quantitative real-time RT-PCR. FABP4 RNA expression was dramatically increased in adipocytes compared to MSCs and osteoblasts. B. MITR inhibits PPARγ-2-activated FABP4 promoter activity. MSCs and 293 cells were transfected with human FABP4 promoter-driven luciferase reporter plasmid (FABP4-P) together with internal control plasmid pRL-TK, PPARγ-2 or MITR plasmids as indicated. The FABP4 promoter-driven reporter luciferase activity was measured by dual-luciferase reporter assay system. Protein expression of PPARγ-2 or MITR was analyzed using western blotting with antibodies as indicated. C. MITR blocks binding of PPARγ-2 to the human FABP4 promoter. MSCs were transfected with PPARγ-2, MITR or vector control pcDNA3.1 plasmids as indicated. Cross-linked chromatin was immunoprecipitated using PPARγ-2 or IgG antibodies. The input and

14

immunoprecipitated DNA were subjected to real time PCR using primers corresponding to promoter region of FABP4 listed in supplemental Table 1. D. PPARγ-2 and RUNX2 specifically bind to FABP4 or OPN promoter in adipocytes and osteoblasts, respectively. Cross-linked chromatin from Ost. or Adi. was immunoprecipitated using PPARγ-2, RUNX2 or IgG antibodies. The input and immunoprecipitated DNA were subjected to PCR or real time PCR using primers corresponding to promoter regions of FABP4 (top panel) or OPN (bottom panel) listed in supplemental Table 1. E. Model for EZH2-MITR mediated MSC differentiation into osteoblasts and adipocytes. EZH2 binds to the MITR promoter and inhibits MITR expression in adipocytes but not in osteoblasts. The presence of MITR in osteoblasts promotes MITR interacting with PPARγ-2 in the nucleus of osteoblasts, which interrupts PPARγ-2 transcriptional activity resulting in attenuation of adipogenesis and acceleration of osteogenesis. Values are represented as the mean ± SD. p-values were analyzed using Student's t-test. FABP4, Fatty acid binding protein 4; OPN, osteopontin.
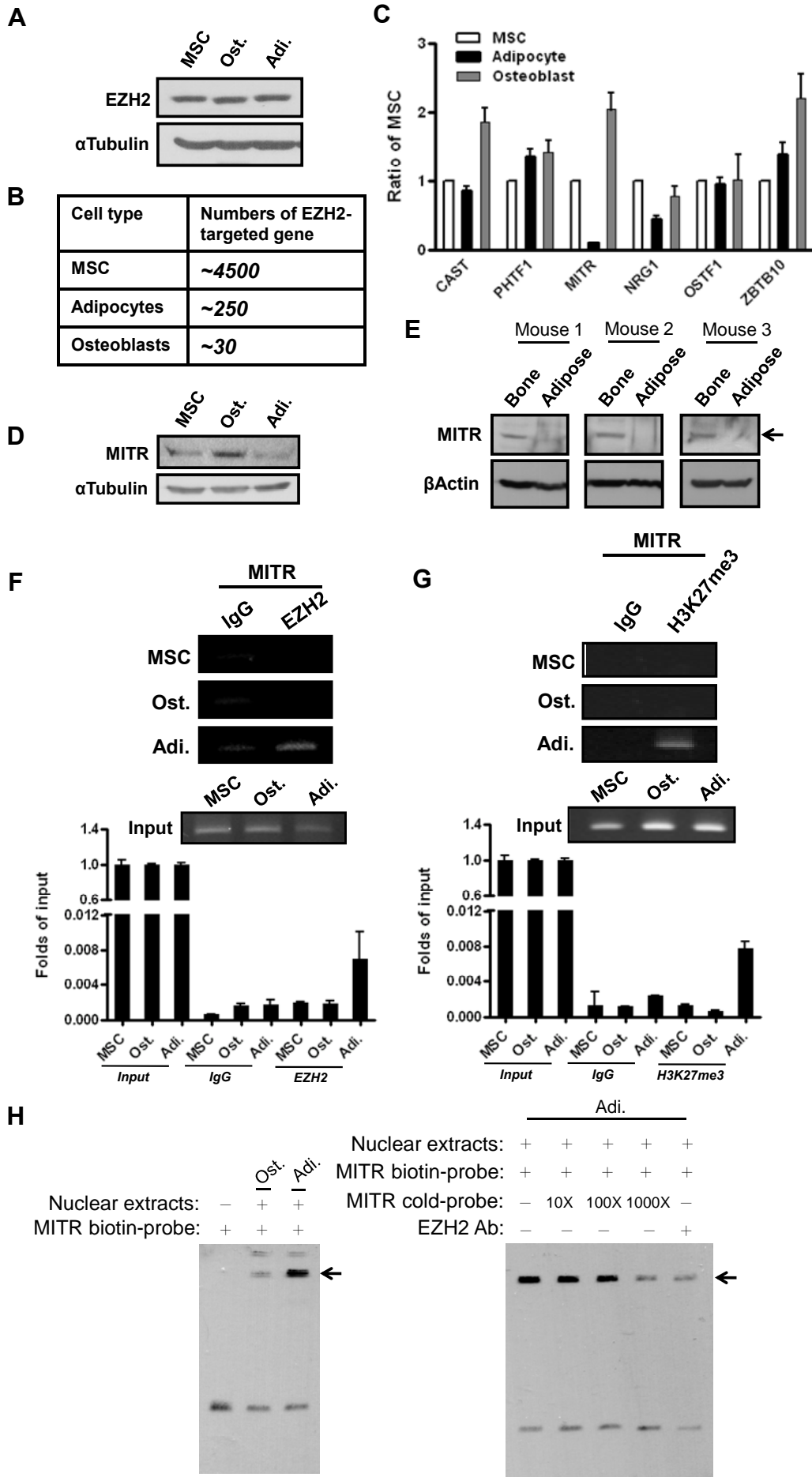
Figure 1, Chen et al.
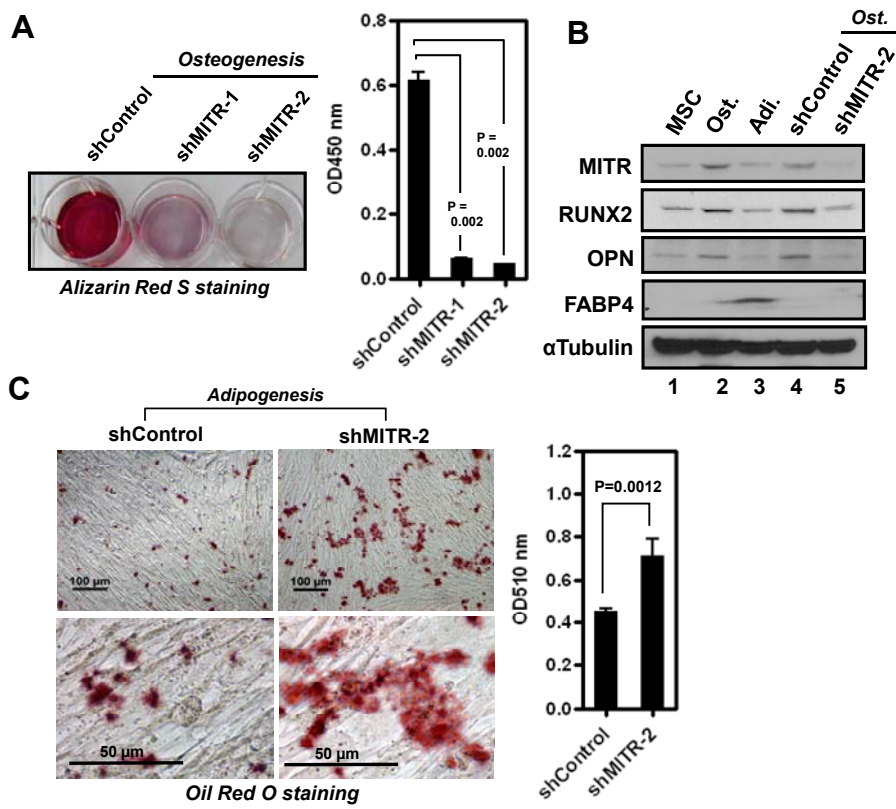
Figure 2, Chen et al.

A Osteogenesis

shControl shMITR-1 shMITR-2

Alizarin Red S staining

B

MITR
RUNX2
OPN
FABP4
αTubulin

MSC Ost. Adi. shControl shMITR-2

Ost.

1 2 3 4 5

C Adipogenesis

shControl shMITR-2

100 µm 100 µm

50 µm 50 µm

Oil Red O staining

P = 0.002

P = 0.002

P=0.0012

Figure 3, Chen et al.

A

MITR

αTubulin

B

Osteogenesis

MSC   AdControl   AdMITR

Alizarin Red S staining

P=
0.007

C

Adipogenesis
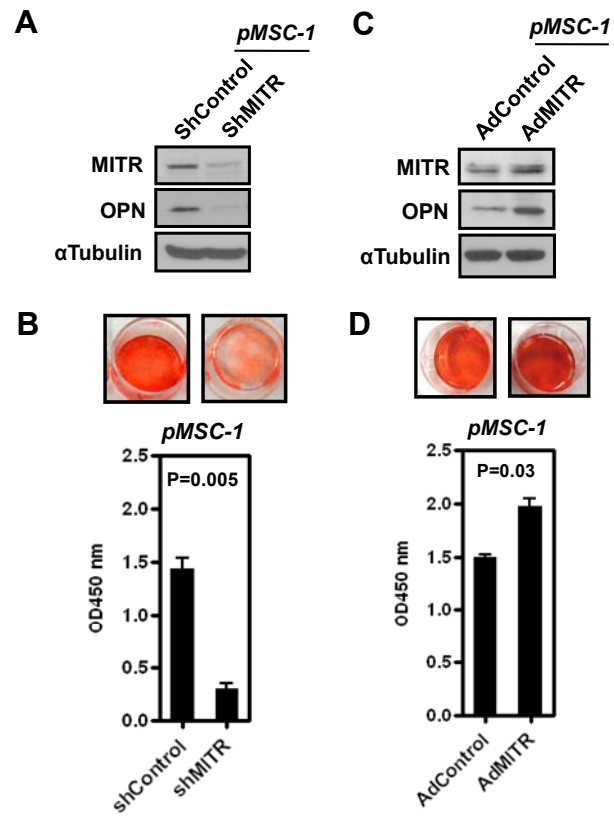
MSC   AdControl   AdMITR

Oil Red O staining

P = 0.042
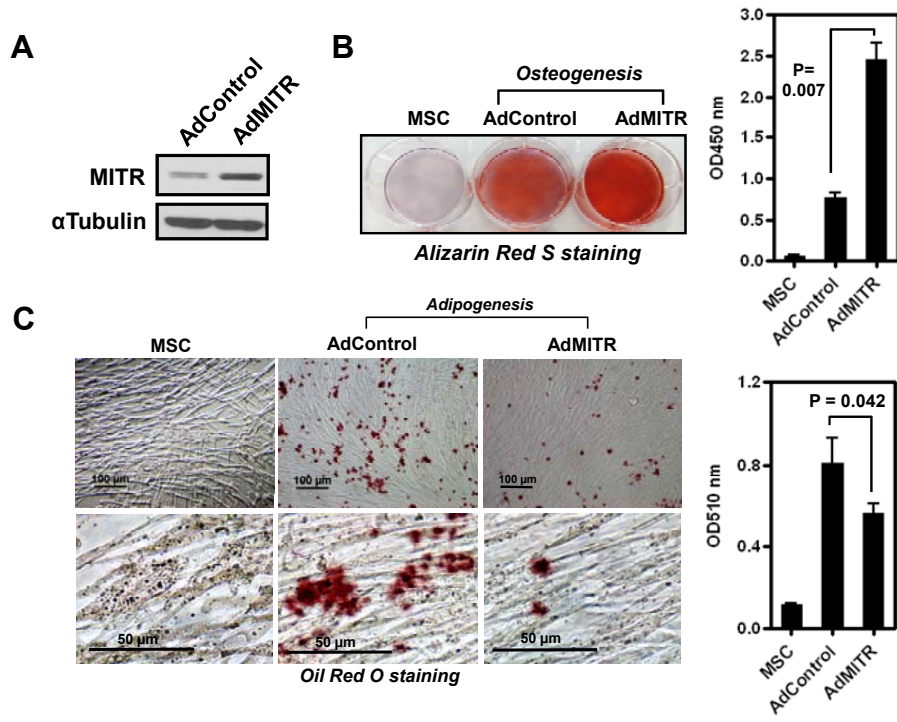
Figure 4, Chen et al.

Figure 5, Chen et al.

A

Nuclear: Ost.

IP: IgG MITR

PPARγ-2 ← PPARγ-2
← Heavy chain

MITR

Cytosol: Ost.

IP: IgG MITR

PPARγ-2 ← Heavy chain

MITR

B

Nuclear: Ost.

IP: IgG PPARγ-2

MITR ←

PPARγ-2

Cytosol: Ost.

IP: IgG PPARγ-2

MITR

PPARγ-2

C

Nuclear: Ost.

IP: IgG MITR

RUNX2

MITR

Cytosol: Ost.

IP: IgG MITR

RUNX2

MITR

Figure 6, Chen et al.